

MILA: Multi-Task Learning from Videos via Efficient Inter-Frame Local Attention

Donghyun Kim¹, Tian Lan², Chuhan Zou², Ning Xu²,
Bryan A. Plummer¹, Stan Sclaroff¹, Jayan Eledath², Gerard Medioni²
¹Boston University, ²Amazon

¹{donhk, bplum, sclaroff}@bu.edu, ²{tianlan, ninxu, zouchuha, eledathj, medioni}@amazon.com

Abstract

Prior work in multi-task learning has mainly focused on predictions on a single image. In this work, we present a new approach for multi-task learning from videos via efficient inter-frame local attention (MILA). Our approach contains a novel inter-frame attention module which allows learning of task-specific attention across frames. We embed the attention module in a “slow-fast” architecture, where the slower network runs on sparsely sampled keyframes and the light-weight shallow network runs on non-keyframes at a high frame rate. We also propose an effective adversarial learning strategy to encourage the slow and fast network to learn similar features. Our approach ensures low-latency multi-task learning while maintaining high quality predictions. Experiments show competitive accuracy compared to state-of-the-art on two multi-task learning benchmarks while reducing the number of floating point operations (FLOPs) by up to 70%. In addition, our attention based feature propagation method (ILA) outperforms prior work in terms of task accuracy while also reducing up to 90% of FLOPs.

1. Introduction

Computer vision applications, such as autonomous driving and indoor navigation, require multi-task predictions from video streams. For example, a self-driving system needs semantic segmentation at each time frame to understand what entities are around the car, and depth estimation to determine how far away each entity is. This makes multi-task learning methods ideal since their shared representation can boost performance on each task while also being more computationally efficient.

In this paper, we focus on efficient multi-task learning for dense pixel-wise predictions (e.g. semantic segmentation and depth estimation) by leveraging a monocular video. Figure 1 compares the performances and computational

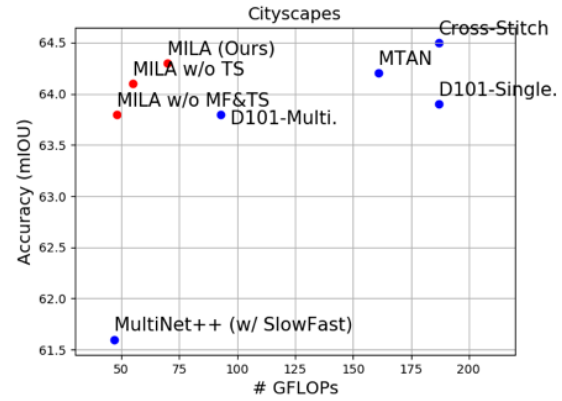


Figure 1: Comparison of multi-task learning methods on the number of GFLOPs and mIoU performance on the Cityscapes dataset. Our method (MILA) reduces computational burden significantly while maintaining accuracy. Our ILA module can be extended to attend task-specific (TS) and multi-frame features (MF) with minimal computations. Please refer to the notation of each compared method and baseline in Sec. 4.2.

burden tradeoffs between existing multi-task learning methods (blue) and our method (red). Recent multi-task learning approaches for dense predictions are mainly single-frame based [13, 26, 29, 22] and often involve heavy task-specific layers (illustrated in Figure 2(a-b)), or a naive concatenation of the features from two consecutive frames from a video [4] (Figure 2(c)), which require a massive number of floating point operations (FLOPs) to compute. To address this drawback, we propose the multi-task learning from videos via efficient inter-frame local attention (MILA) to exploit temporal cues using inter-frame local attention (ILA) modules as shown in Figure 2(d). Different from existing attention modules that only attend features in the current single-frame [26, 11], ILA efficiently learns to attend and propagate features from the previous frames. ILA

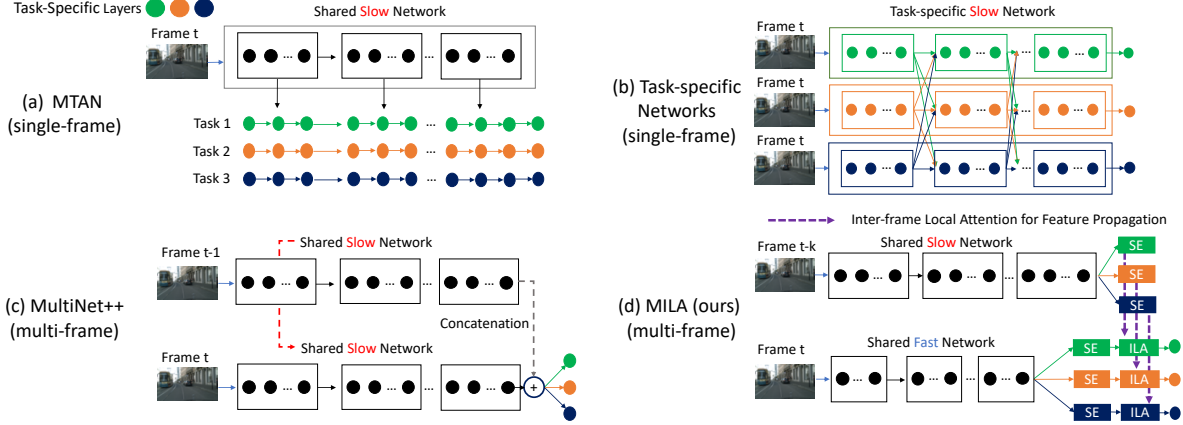


Figure 2: An illustration of difference between previous multi-task learning models and our multi-task model, MILA. Previous methods use only a *Slow* network (e.g. ResNet101) for every frame ((a), (b), and (c)) and heavy task-specific layers for each task ((a) and (b)), which requires massive computations. In (d), we propose an efficient approach for multi-task learning from videos by utilizing a *Fast* network (e.g. ResNet18) for non-keyframes and propagating the previous keyframe features from the *Slow* network via our inter-frame local attention module (ILA). ILA is light-weight, accurate, and extended task-specific attention modules without requiring massive computations.

is light-weight as compared to the expensive optical-flow based feature warping which is widely used in previous works [21, 40]. In addition, the performance of optical flow warping based methods can be affected by the quality of estimated optical flow, which may fail on fast motion or occluded objects. MILA architecture utilizes the *SlowFast* framework [21, 10], which shows superiority in reducing computational cost while maintaining comparable accuracy. In the *SlowFast* architecture, keyframes are processed by a deep (*Slow*) network, and non-keyframes are processed by a shallow (*Fast*) network. Unlike the previous task-specific heavy layers, we show improvements in accuracy with our light-weight task-specific attention based ILA by leveraging temporal cues, and a novel adversarial learning strategy that encourages similar feature representations for both the *Slow* and *Fast* network. The major difference from previous attention modules (e.g. [11]) is that our attention module performs on inter-frame features from different networks, which is a challenging problem that is not fully addressed by the existing attention modules. Figure 2 illustrates the difference between our approach (MILA) and existing multi-task learning methods.

We evaluate our approach on two standard multi-task learning benchmarks: the Cityscapes dataset [5] with outdoor scenes and the NYUd v2 dataset [33] with indoor scenes. As shown in Figure 1, MILA method achieves on-par accuracy compared to the state-of-the-art multi-task learning methods, while reducing the number of FLOPs by up to 70%. MILA reduces computational burden by a large margin without compromising accuracy. Moreover, we show that ILA module can be used as a standalone fea-

ture propagation method in videos: it is much faster compared to existing feature propagation methods, and more accurate than the state-of-the-art [21, 25] on semantic video segmentation in our experiments.

Our contributions are :

- We address the task of video-based multi-task learning, which is not well explored in previous work. We present a multi-task learning via inter-frame local attention (MILA) that achieves competitive accuracy as compared to the state-of-the-art with largely reduced computational cost.
- We introduce a new inter-frame local attention module (ILA) which learns task-specific features across frames. Our network is trained end-to-end with an adversarial loss.
- Our ILA module can be used as a standalone feature propagation method in video tasks such as semantic segmentation, achieving the top accuracy with up to 90% reduction of FLOPs.

2. Related Work

Multi-task learning (MTL) has shown improved accuracy and increased memory-efficiency for various tasks such as object detection and segmentation [1, 2, 17, 29], joint scene geometry and semantic segmentation [4, 26, 38, 22, 35, 23, 9]. Previous approaches mainly focus on predictions from a single image. Chennupati *et al.* [4] propose to learn from videos by concatenating the features from two consecutive frames. Contrary to prior work, we go beyond

single-frame based prediction and learn from videos by aggregating and propagating features across multiple frames.

Although the shared representation of MTL can help improve generalization and reduce computational costs, it is also shown to potentially hurt accuracy due to the trade-off learning from multiple tasks [28]. Kendall *et al.* [22] propose to use homoscedastic uncertainty to weight different tasks adaptively during training. Sensor and Koltun [32] propose to optimize an upper bound for the multi-objective loss. However, refining the training loss usually has limited improvements as shown in [26]. Other methods introduce complex task-specific layers (*e.g.* task-specific backbone) [26, 29, 31] that also significantly increases the computational burden. In contrast, we show that our lightweight task-specific model design for our inter-frame attention module is able to achieve competitive task accuracy at a much lower computational cost.

Feature propagation has been widely used in video applications to exploit temporal cues across frames [21, 25, 30, 40, 12]. Prior work has introduced methods based on optical flow based warping [40, 21, 12] which largely increases the computational cost with limited improvements in accuracy. Jain *et al.* [21] propose to reduce the inference cost by combining the predictions of two network branches: a deep reference branch that computes detailed features from keyframes, and a shallower update branch that incorporates less detailed features at each frame with the wrapped features from a recently met keyframe. This has the similar spirit as the SlowFast [10] design for video recognition. Li *et al.* [25] further propose to use spatially variant convolution layers for feature propagation which is faster than optical flow warping. Our network, MILA, stems from the spirit of the SlowFast network, and we use our light-weight inter-frame local attention (ILA) module for feature propagation instead of the expensive optical flow based approach. We also perform dense feature propagation between every neighboring frame, in addition to the sparse propagation between keyframes and non-keyframes only.

Attention modules are widely used in various tasks such as natural language processing (NLP) [7, 36], semantic segmentation [20, 24, 36, 11, 39], image classification [19, 37] and action recognition [15, 14]. Vaswani *et al.* [36] propose a self-attention module for a translation task by extracting global dependencies from input sequences. The self-attention first computes feature representations for query, key, and value, then computes global attention weights by measuring the similarity between the query and key. The final value can be obtained by a weighted sum of values from the sequence of input. Fu *et al.* [11] apply the self-attention module for semantic segmentation by attending all pixels given a pixel query in order to capture global relation in a single frame. We reformulate the self-attention mechanism to attend inter-frames from the two different representations

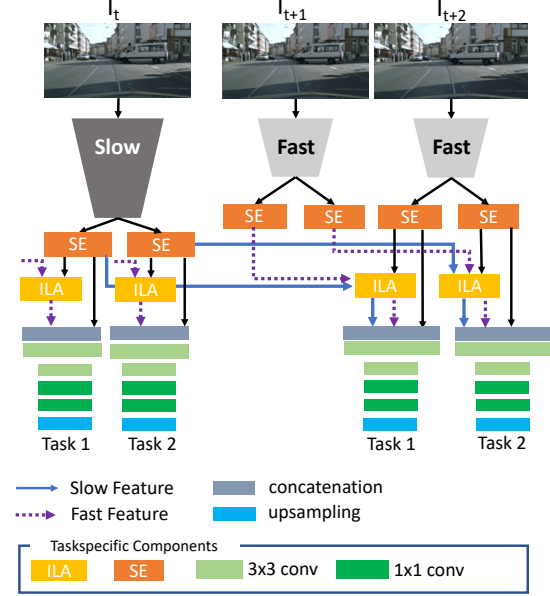


Figure 3: An illustration of our network architecture and the inference step of a keyframe I_t and a non-keyframe I_{t+2} . ILA propagates multi-frame features to the current inference frame.

(from *Slow* and *Fast* network) for efficient and accurate feature propagation.

3. Multi-task Learning via Inter-Frame Local Attention

We propose Multi-task Learning via Inter-Frame Local Attention (MILA), which is a computationally efficient multi-task learning model, with high quality prediction by leveraging temporal cues in video streams. One major challenge is to effectively learn spatial and temporal cues of different tasks in a light-weight and efficient manner. Figure 3 shows the architecture of the proposed network. Inspired by the *SlowFast* network [10, 21], we build an efficient multi-task network with a two-branch design: the *Slow* branch runs on sparsely sampled keyframes and the light-weight *Fast* network runs on non-keyframes. Unlike previous works relying on heavy task-specific layers [26, 29], we also introduce a new light-weight task-specific attention module to learn and propagate task-specific features across frames.

In the following, we first explain our multi-task network architecture (MILA) in Sec. 3.1. Then, we introduce our novel task-specific inter-frame local attention (ILA) module in Sec. 3.2, and an adversarial loss that further boosts the overall performance in Sec. 3.3.

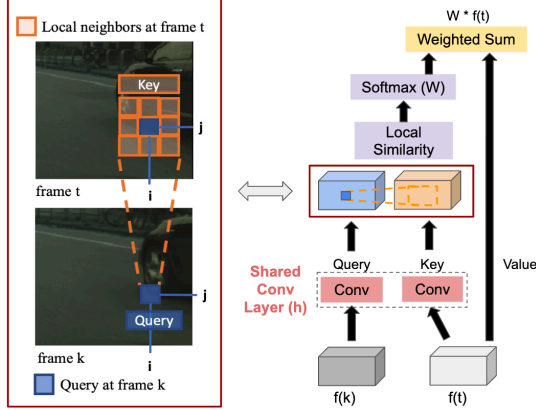


Figure 4: Inter-frame local attention (ILA) accounts for motion by finding local attention weights in inter-frames. With a shared conv layers, our module generates high attention weights on the similar features between frames.

3.1. Architecture Overview

MILA consists of two components: 1) a shared encoder network: a *Slow* network that operates on sparsely sampled keyframes; a *Fast* network runs on other frames. 2) M task-specific decoder networks, one for each task. Each decoder network learns to attend to task-specific features from previous frames that it propagates to the current frame before carrying out pixel-level prediction of semantic entities as well as performing depth estimation.

The input is a sequence of N RGB frames $I = \{I_1, I_2, \dots, I_N\}$ from a monocular video, and the output is pixel-level predictions on M tasks, $Y = \{y_1, y_2, \dots, y_M\}$. At each time step $t \in \{1, 2, \dots, T\}$, we encode frame I_t using the *Slow* network if it's a keyframe, and the *Fast* network otherwise. In our implementation, we use ResNet-101 as the *Slow* network and ResNet-18 as the *Fast* network. The encoder is shared among all tasks. We use $Slow(I_t)$ to denote features encoded by the *Slow* network and $Fast(I_t)$ for features encoded by the *Fast* network.

At the decoder step, we perform predictions on each task with a task-specific decoder $\{D_1, D_2, \dots, D_M\}$, where M is the total number of tasks. Each task-specific decoder consists of squeeze-excitation (SE) blocks on top of shared features from the encoder, inter-frame local attention (ILA) modules to extract and propagate task-specific features across frames and a set of conv layers. In order to fully leverage temporal information, we enable multi-frame feature propagation: a non-keyframe receives features propagated from the last keyframe and the last non-keyframe; a keyframe receives features propagated from the last non-keyframe. This is different from existing feature propagation [21, 25] which only propagates features from a keyframe to a non-keyframe.

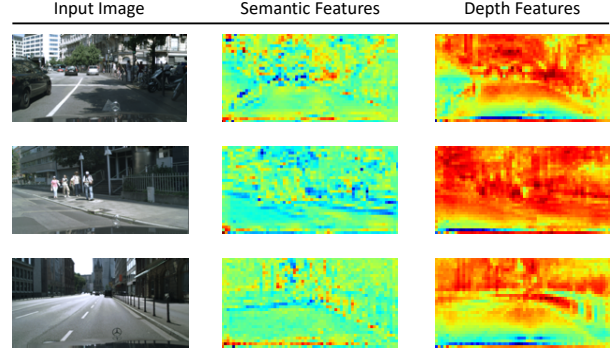


Figure 5: Visualization of task-specific features from our task-specific attention module.

3.2. Inter-Frame Local Attention (ILA)

The key challenge for attention based feature propagation is how to leverage inter-frame temporal cues to propagate features efficiently and effectively. We introduce a light-weight inter-frame local attention (ILA) module for feature propagation. As illustrated in Figure 4, ILA computes local attention weights W from the feature maps of two different frames (either two neighboring frames or a non-keyframe and a keyframe) to exploit local motion changes.

Given a pair of frames I_t and I_k , ILA operates on feature maps f_t and f_k and propagates features from f_t to f_k . In our design (see Figure 3), the feature maps are the output of task-specific squeeze-and-excitation (SE) blocks [19]. For each pixel on the feature map f_k , we propagate the features from f_t based on a weighted combination of pixels in a local neighborhood.

$$f_{t \rightarrow k}(i, j) = \sum_{x=-L/2}^{L/2} \sum_{y=-L/2}^{L/2} W_{i,j}(x, y) f_t(i+x, j+y) \quad (1)$$

where (i, j) denotes the pixel location in the image, L is the window size and W is the attention weight obtained by measuring the similarity between the two feature maps f_t and f_k . The attention weight matrix W is defined in the following:

$$W_{i,j}(x, y) = \text{softmax}(h(f_k(i, j)) \cdot h(f_t(i+x, j+y))) \quad (2)$$

where $W_{i,j}(x, y)$ is the attention weight which measures the similarity between features at position (i, j) and $(i+x, j+y)$ of the two feature maps, respectively. h is a 3×3 convolution layer shared between the two feature maps to capture the semantic information in a local window around pixel (i, j) . We use inner product to capture the similarities. Then a softmax layer is applied to ensure the sum of weights equals to 1. Note that ILA is performed only on lo-

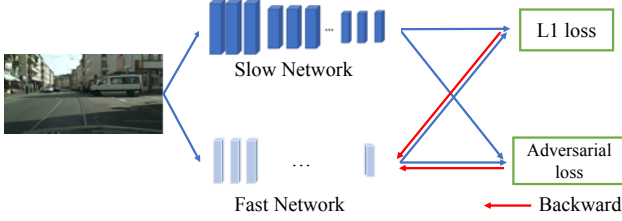


Figure 6: Adversarial learning. In order to let our attention module (ILA) capture temporal consistency, we adopt an adversarial learning strategy for training, where we use a combination of L1 and adversarial loss for the *Fast* network to mimic the features learned by the *Slow* network.

cal neighborhoods, resulting in reduced computational cost as compared to existing global attention modules [11].

Task-specific Attention. A common challenge in multi-task learning is on how to balance the shared and task-specific features. A heavily shared representation can reduce computational costs and can help prevent over-fitting, but it can also hurt accuracy due to limited model capacity to handle multiple tasks [28]. To solve this issue, methods that add extra task specific layers to the multi-task network [26, 29, 31] gained popularity during the recent years and achieved higher task accuracy. The drawback is that the complex task-specific layers also significantly increase computational burden.

Our ILA module is task-specific in order to learn discriminative task-specific features. In contrast to prior work, ILA learns to select and propagate features from previous frames rather than attending the features in the current frame. Leveraging temporal information drastically reduces the required complexity of task-specific layers as the model capacity and discriminative power are shared across multiple frames. Unlike the previous heavy attention modules in [26, 11], the other advantage is that ILA only attends to features from the task-specific SE blocks within a local window from previous frames only at the last layer of the backbone. This assumption on temporal consistency reduces the computational cost of ILA. Compared to state-of-the-art attention-based multi-task network [26], MILA achieves better accuracy with 54% reduction of FLOPs.

Visualization of the learned task-specific features are shown in Figure 5. We can see clear differences in feature patterns for different tasks. Semantic segmentation features highlight object patches, lines and boundaries, while the depth features highlight foreground and background. This confirms the effectiveness of ILA as a feature selector to focus on parts that are discriminative for each task.

3.3. Boosting ILA for *SlowFast*

ILA assumes similar features propagate across frames. The high-level idea is similar to optical flow which assumes color constancy between pixels in consecutive images in order to capture motion. However, different backbones (e.g. ResNet-101 and ResNet-18) from the *Slow* and *Fast* branches cannot guarantee learning similar features for similar image patches, where naive attention modules could not improve accuracy in our experiments.

We adopt adversarial learning to train the network so that the *Fast* network learns similar features to the more accurate *Slow* network. Figure 6 illustrates our approach. Our approach is inspired by GANs [16], where a discriminator D is trained to classify whether the features are output of the *Slow* network or the *Fast* network, and the *Fast* network is trained to confuse the discriminator by "mimicking" the output features of the *Slow* network. In practice, we observed combining L1 loss with the adversarial loss lead to improved accuracy. Our loss function \mathcal{L} is defined in the following:

$$\begin{aligned}\mathcal{L} &= \min(\alpha\mathcal{L}_{L1} - \beta \min_D \mathcal{L}_{adversarial}) \\ \mathcal{L}_{L1} &= |Slow(I_t) - Fast(I_t)| \\ \mathcal{L}_{adversarial} &= \log D(Slow(I_t)) + \log(1 - D(Fast(I_t)))\end{aligned}\quad (3)$$

where $Slow(I_t)$ and $Fast(I_t)$ are the features of the *Slow* and *Fast* backbone networks on image I_t . The loss function L enforces the *Fast* network to mimic the features learned from the *Slow* network.

4. Experiments

We validate our approach (MILA) in the following two aspects for both accuracy and computation cost. (1) Comparison with the state-of-the-art multi-task learning approaches on videos, the ablation study for our proposed task-specific attention module and our training losses. (2) The efficacy of our attention based feature propagation approach (ILA) compared with other feature propagation methods.

4.1. Implementation Details

We implement MILA using PyTorch. We train MILA using ADAM optimizer with $\beta_1 = 0.9$ and $\beta_2 = 0.99$. The learning rate is $1e^{-4}$ and batch size is 4. The training loss converges after 50 epochs. For the adversarial loss in Eq. 3, we set $\alpha = \beta = 1$. ILA computes on a window size of $L = 5$ in Eq. 2. We use DeepLab-ResNet101 [3, 27, 18] as our *Slow* network and DeepLab-ResNet18 as our *Fast* Network. The backbones are pre-trained on ImageNet [6] and finetuned for multi-task learning. For brevity, Deeplab-ResNet101 is denoted as **D101**. **D101-18** refers to the

Model	Segmentation		Depth		Normal Estimation					GFLOPs
					Angle Dist. ↓		Angle° Within ↑			
	mIOU ↑	Acc. ↑	Abs. ↓	Rel. ↓	Mean	Median	11.25°	22.5°	30.0°	
D101-SingleTask	37.2	75.0	39.3	16.6	22.8	16.6	35.7	62.8	73.9	236
D101-MultiTask	37.1	75.3	39.0	16.3	23.7	17.6	34.0	60.2	71.7	79
MTAN-Seg. [26]	17.7	55.3	59.0	25.8	31.4	25.4	23.2	45.7	57.6	178
Cross-Stitch-Seg. [26]	14.7	50.2	64.8	28.7	33.6	28.6	20.1	40.5	52.0	213
MTAN*	37.1	74.3	40.0	16.9	23.9	18.1	33.5	59.5	70.4	151
Cross-Stitch*	37.5	74.5	39.5	16.2	22.7	16.5	36.8	63.0	73.8	236
MultiNet++* [4]	32.8	73.1	41.1	17.3	24.4	18.1	33.4	58.9	70.2	40
MILA (Ours)	38.1	75.1	38.6	16.1	23.2	17.0	35.4	61.8	72.5	70

Table 1: Comparisons for video based Multi-task learning on NYUd v2 dataset. * means training with the same Deeplab-ResNet101 backbone as ours. D101 denotes the Deeplab-ResNet101 backbone. Cross-stitch* shows better results in the normal estimation task mostly because it contains task-specific backbones.

SlowFast network with DeepLab-ResNet101 and DeepLab-ResNet18. Each task-specific decoder consists of three convolution layers with kernel size of 3x3, 1x1 and 1x1 respectively, and feature size of 512 and 256 in between. To compare ILA with other feature propagation methods, we directly train our network for the single task of semantic video segmentation.

Keyframe Interval. We train our network with a fixed keyframe interval of $K = 5$ following [21] (every 5-th frame is a keyframe). For evaluation, since frames in a video are sparsely annotated (e.g. 20-th frame in a video clip) in existing datasets, we measure performances of an annotated frame by running our method for all possible keyframe interval offsets $[0, K - 1]$ and report the averaged accuracy and GFLOPs. For the evaluation of ILA on semantic video segmentation, we use the same keyframe intervals as the compared methods (5 and 10).

4.2. Setup

Datasets. We evaluate our MILA on two widely used public video datasets: Cityscapes [5] and NYUd v2 [33]. We follow the evaluation protocols as in Liu *et al.* [26]: on Cityscapes, we perform 2 *task predictions* including 7-class segmentation and depth estimation, where images are resized to 256×512 to boost up training process; on the NYUd v2 dataset, we perform 3 *task predictions* including 13-class segmentation, depth estimation and normal estimation, with input images resized to 288×384 . For evaluation of ILA on the single task of semantic video segmentation, we perform 19-class segmentation the same as the state-of-the-art by Jain *et al.* [21].

Metrics. For semantic segmentation, we use mean intersection-over union (mIoU) metric and pixel accuracy (PA). For depth estimation, we evaluate on absolute and relative depth errors from the ground truth. For normal estimation, we measure the mean and median angle distances between the predicted angles and ground-truth angles. We

also measure the percentage of pixels that are within the angles of 11° , 22.5° , 30° to the ground-truth. We compare on computation cost based on GFLOPs following [10, 41, 34] and use the thop library¹ for counting GFLOPs.

Baselines. We compare with state-of-the-art multi-task learning approaches: **MTAN** [26], **Cross-Stitch** network [29] and **MultiNet++** [4]. MTAN and Cross-Stitch are single frame based, while MultiNet++ uses multi-frame as input. Since the original proposed MTAN and Cross-Stitch use different backbones, for fair comparison, we report performance of the two using the same DeepLab-ResNet101 backbone as our *Slow* network (which shows better performance than using the backbone mentioned in their papers). We use the four outputs of each group of layers containing the residual blocks in the backbone as input for the attention modules for the two methods (see Figure 2). For our method and MultiNet++, we use the SlowFast network with ResNet101 and ResNet18. We also compare with two other baselines: **D101-SingleTask**, which uses a separate ResNet101 backbone for training each task without any shared features; **D101-MultiTask**, which uses the shared ResNet101 backbone with task-specific decoders.

4.3. Video Based Multi-Task Learning

We report the performance of video based multi-task learning on the NYUd v2 dataset in Table 1 and the Cityscapes dataset in Table 2 respectively. We show in Figure 7 sample qualitative results from the Cityscapes dataset. Please check more results and analyses in our supplementary material.

In Table 1, on the NYUd v2 dataset, we outperform other approaches for depth estimation and one metric of mIOU for semantic segmentation, with ranked 2nd segmentation accuracy. MILA shows slightly worse performance for normal estimation than Cross-Stitch. This is because Cross-Stitch has task-specific backbones, while MILA use

¹<https://github.com/Lyken17/pytorch-OpCounter>

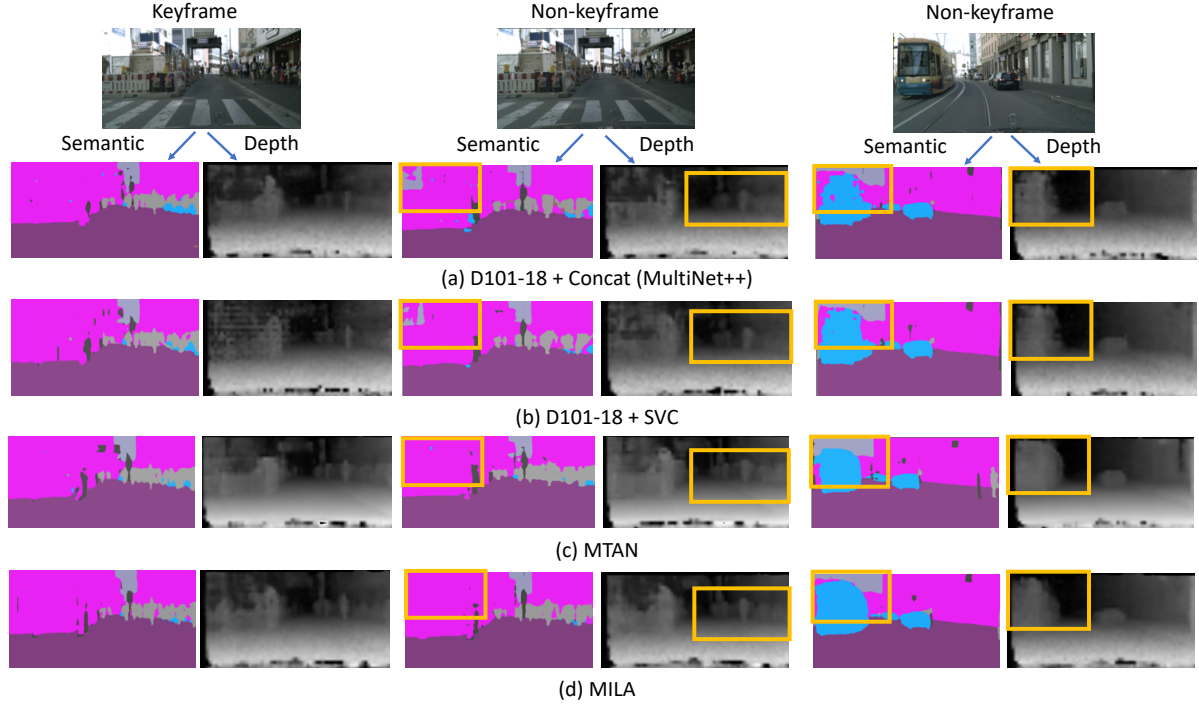


Figure 7: Qualitative results for video based multi-task learning on Cityscapes dataset. We choose the two frames in a video, where the first image is a keyframe and the second image is non-keyframe with offset 4. For the keyframe, the three methods produce very similar qualitative results. For non-keyframes, the baseline methods (a, b) performs worse (see orange boxes) but our method (b) still obtains robust to the non-keyframes.

Model	Segmentation		Depth		GFLOPs
	mIOU \uparrow	Acc. \uparrow	Abs. \downarrow	Rel. \downarrow	
D101-SingleTask	63.9	94.4	1.02	25.3	187
D101-MultiTask	63.8	94.4	1.06	31.9	93
MTAN-SegNet [26]	53.0	91.1	1.44	33.6	168
MTAN *	64.2	94.5	1.06	26.3	161
Cross-Stitch*	64.5	94.5	1.04	33.0	187
MultiNet++ [4]	61.6	93.9	1.08	28.5	47
MILA w/o MF&TS	63.8	94.4	1.05	32.9	48
MILA w/o TS	64.1	94.5	1.03	31.5	55
MILA (Ours)	64.3	94.6	1.02	25.2	70

Table 2: Comparison for video based multi-task learning on the Cityscapes dataset. * means training with the same Deeplab-ResNet101 backbone. Ours and MultiNet++ uses the D101-18 backbone.

a single shared one, which is significantly computationally efficient, saving 70% of computational costs (236 vs. 70 GFLOPs) compared to Cross-Stitch [29]. MILA also saves 46% (70/151 GFLOPs) of computations compared to MTAN [26] as shown in Table 1 by replacing task-specific heavy layers with light-weight task-specific ILAs. We rank the 2nd for GFLOPs right after MultiNet++ but with much

Backbone	L1	Adv.	ILA	mIOU (\uparrow)	Depth Err. (\downarrow)
D101-18				61.6	1.08
D101-18	✓			61.8	1.07
D101-18			✓	61.9	1.08
D101-18	✓		✓	63.3	1.05
D101-18	✓	✓	✓	63.8	1.05

Table 3: Ablation study of ILA on Cityscapes. ILA combined with L1 loss and adversarial loss (denoted by Adv.) leads to clear improvement. ILA without the proposed losses obtains similar performances as just simple concatenation [4].

better accuracy. In Table 2, MILA outperforms all other methods for depth estimation and achieves the the best accuracy for semantic segmentation, while ranking the 2nd for mIOU on Cityscapes.

Ablation study. The last three rows in Table 2 show the ablation study of MILA method. “MILA w/o TS” means our approach without task-specific attention design. “MILA w/o MF&TS” means without both task-specific design and feature propagation for neighboring frames. “MILA w/o MF&TS” achieves similar performance as D101-MultiTask while saving 48% computations. MILA outperforms D101-MultiTask and reduces 25% of compu-

Backbone	Window Size	mIOU (\uparrow)	Depth Err. (\downarrow)
D101-18	3x3	64.1	1.02
D101-18	5x5	64.3	1.02
D101-18	7x7	64.2	1.02
D101-18	Global	62.4	1.10

Table 4: Ablation study on the kernel size in ILA module on Cityscapes. ILA performs better than global attention for feature propagation.

Backbone	K	Feature Prop.	mIOU (%)
D101-18	5	Optical flow	72.1
D101-18	5	ILA (Ours)	73.2
D101-18	10	Optical flow	69.8
D101-18	10	ILA (Ours)	72.1
D101-34	5	Optical flow	72.4
D101-34	5	ILA (Ours)	74.3
D101-34	10	Optical flow	70.1
D101-34	10	ILA (Ours)	73.8

Table 5: Comparison with optical-flow based feature propagation [21] for the semantic segmentation task on Cityscapes. A keyframe interval is denoted by K .

tations. MILA approach shows the best performed accuracy with a small increase in GFLOPs.

We show the ablation study on our inter-frame local attention (ILA). Table 3 reports the impact of the adversarial and L1 losses (Eq. 3). In the third line of Table 3, it shows that the ILA alone does not greatly improve the performances. However, when ILA is combined with the proposed losses, it significantly increases the accuracy. In addition, we show the ablation study for the local window size in Table 4. ILA is not sensitive to small changes in the window size, but performance drops significantly when the window size is global.

4.4. Detailed Analysis on Feature Propagation

We compare ILA with the two feature propagation methods: (1) optical flow based warping with FlowNet-S [8], which shows state-of-the-art performance on the single task of semantic video segmentation for the Accel method [21] and (2) spatially variant [25] (SVC) also for semantic video segmentation. We use the same backbone for all methods for fair comparisons.

Performance comparison. To compare with optical flow based warping [21], we follow their semantic segmentation evaluation protocol as shown in Table 5. Feature propagated with ILA obtains higher accuracy than the method based on optical flow warping [21]. We observe that the accuracy improvements of ILA are more evident in the higher keyframe interval.

Feature Prop.	Segmentation		Depth	
	mIOU \uparrow	Acc. \uparrow	Abs. \downarrow	Rel. \downarrow
(a) Cityscapes				
SVC [25]	62.3	94.0	1.06	33.3
ILA (Ours)	63.8	94.4	1.05	32.9
(b) NYUv2				
SVC [25]	35.7	74.7	40.3	17.0
ILA (Ours)	36.6	74.8	39.2	16.5

Table 6: Comparison with for feature propagation methods with D101-18 backbone on Cityscapes and NYUv2

Feature Propagation	GFLOPs	# Conv.	# Param
(a) Input size: 258×512			
Optical flow [21, 8]	7.5	23	38M
SVC [25]	5.4	3	3M
ILA (Ours)	0.2	1	0.2M
(b) Input size: 1024×2048			
Optical flow [21, 8]	71.2	23	38M
SVC [25]	108	3	3M
ILA (Ours)	5.4	1	0.2M

Table 7: Comparison on feature propagation modules. SVC represents the method of [25]. Our method is light-weight and computationally efficient.

In Table 6, we provide comparisons with [25] on Cityscapes and NYUd v2 on multi-task learning. ILA method outperforms other method in the two datasets with less computational burden. We observe that the quality of optical flow estimation is bad in this evaluation protocol (*i.e.* low-resolution images), so the optical flow warping based feature propagation performs worse.

Space and computation cost. In Table 7, we show the comparison of GFLOPs, number of convolutional layers and number of parameters for the optical flow warping, SVC and our ILA. We report numbers given different input sizes. ILA consists of only one convolutional layer, making it much more memory efficient than the other two methods. For GFLOPs, other methods require more computations than ILA and the gain is more evident when the input size is larger. ILA takes only 4% (0.2/5.4 GFLOPs) of computations in the SVC feature propagation [25]. Additional analyses can be found in our supplementary material.

5. Conclusion

We present an efficient and effective multi-task learning framework on video streams. We propose a novel task-specific inter-frame local attention (ILA) module, which accounts for motion and propagate discriminative task-specific features over time in a spatial-variant manner. Our attention module is much faster, more accurate, and modular compared to prior feature propagation methods. While

previous multi-task learning models require heavy computations to extract task-specific features, we show that our inter-frame local attention module can be used to extract task-specific features with minimal computation. Our experiments show that our method significantly reduces the computational cost without compromising accuracy compared to the state-of-the-art multi-task learning models.

References

- [1] Kai Chen, Jiangmiao Pang, Jiaqi Wang, Yu Xiong, Xiao-xiao Li, Shuyang Sun, Wansen Feng, Ziwei Liu, Jianping Shi, Wanli Ouyang, et al. Hybrid task cascade for instance segmentation. In *Proceedings of the IEEE Conference on Computer Vision and Pattern Recognition*, pages 4974–4983, 2019.
- [2] Liang-Chieh Chen, Alexander Hermans, George Papandreou, Florian Schroff, Peng Wang, and Hartwig Adam. Masklab: Instance segmentation by refining object detection with semantic and direction features. In *Proceedings of the IEEE Conference on Computer Vision and Pattern Recognition*, pages 4013–4022, 2018.
- [3] Liang-Chieh Chen, George Papandreou, Iasonas Kokkinos, Kevin Murphy, and Alan L Yuille. Deeplab: Semantic image segmentation with deep convolutional nets, atrous convolution, and fully connected crfs. *IEEE transactions on pattern analysis and machine intelligence*, 40(4):834–848, 2017.
- [4] Sumanth Chennupati, Ganesh Sistu, Senthil Yogamani, and Samir A Rawashdeh. Multinet++: Multi-stream feature aggregation and geometric loss strategy for multi-task learning. In *Proceedings of the IEEE Conference on Computer Vision and Pattern Recognition Workshops*, pages 0–0, 2019.
- [5] Marius Cordts, Mohamed Omran, Sebastian Ramos, Timo Rehfeld, Markus Enzweiler, Rodrigo Benenson, Uwe Franke, Stefan Roth, and Bernt Schiele. The cityscapes dataset for semantic urban scene understanding. In *Proceedings of the IEEE conference on computer vision and pattern recognition*, pages 3213–3223, 2016.
- [6] Jia Deng, Wei Dong, Richard Socher, Li-Jia Li, Kai Li, and Li Fei-Fei. Imagenet: A large-scale hierarchical image database. In *2009 IEEE conference on computer vision and pattern recognition*, pages 248–255. Ieee, 2009.
- [7] Yuntian Deng, Yoon Kim, Justin Chiu, Demi Guo, and Alexander Rush. Latent alignment and variational attention. In *Advances in Neural Information Processing Systems*, pages 9712–9724, 2018.
- [8] Alexey Dosovitskiy, Philipp Fischer, Eddy Ilg, Philip Hausser, Caner Hazirbas, Vladimir Golkov, Patrick Van Der Smagt, Daniel Cremers, and Thomas Brox. FlowNet: Learning optical flow with convolutional networks. In *Proceedings of the IEEE international conference on computer vision*, pages 2758–2766, 2015.
- [9] David Eigen and Rob Fergus. Predicting depth, surface normals and semantic labels with a common multi-scale convolutional architecture. In *Proceedings of the IEEE international conference on computer vision*, pages 2650–2658, 2015.
- [10] Christoph Feichtenhofer, Haoqi Fan, Jitendra Malik, and Kaiming He. Slowfast networks for video recognition. In *Proceedings of the IEEE International Conference on Computer Vision*, pages 6202–6211, 2019.
- [11] Jun Fu, Jing Liu, Haijie Tian, Yong Li, Yongjun Bao, Zhiwei Fang, and Hanqing Lu. Dual attention network for scene segmentation. In *Proceedings of the IEEE Conference on Computer Vision and Pattern Recognition*, pages 3146–3154, 2019.
- [12] Raghudeep Gadde, Varun Jampani, and Peter V Gehler. Semantic video cnns through representation warping. In *Proceedings of the IEEE International Conference on Computer Vision*, pages 4453–4462, 2017.
- [13] Yuan Gao, Jiayi Ma, Mingbo Zhao, Wei Liu, and Alan L Yuille. Nddr-cnn: Layerwise feature fusing in multi-task cnns by neural discriminative dimensionality reduction. In *Proceedings of the IEEE Conference on Computer Vision and Pattern Recognition*, pages 3205–3214, 2019.
- [14] Rohit Girdhar, Joao Carreira, Carl Doersch, and Andrew Zisserman. Video action transformer network. In *Proceedings of the IEEE Conference on Computer Vision and Pattern Recognition*, pages 244–253, 2019.
- [15] Rohit Girdhar and Deva Ramanan. Attentional pooling for action recognition. In *Advances in Neural Information Processing Systems*, pages 34–45, 2017.
- [16] Ian J. Goodfellow, Jean Pouget-Abadie, Mehdi Mirza, Bing Xu, David Warde-Farley, Sherjil Ozair, Aaron C. Courville, and Yoshua Bengio. Generative adversarial nets. In *NIPS*, 2014.
- [17] Kaiming He, Georgia Gkioxari, Piotr Dollár, and Ross Girshick. Mask r-cnn. In *Proceedings of the IEEE international conference on computer vision*, pages 2961–2969, 2017.
- [18] Kaiming He, Xiangyu Zhang, Shaoqing Ren, and Jian Sun. Deep residual learning for image recognition. In *The IEEE Conference on Computer Vision and Pattern Recognition (CVPR)*, June 2016.
- [19] Jie Hu, Li Shen, and Gang Sun. Squeeze-and-excitation networks. In *Proceedings of the IEEE conference on computer vision and pattern recognition*, pages 7132–7141, 2018.
- [20] Zilong Huang, Xinggang Wang, Lichao Huang, Chang Huang, Yunchao Wei, and Wenyu Liu. Ccnet: Criss-cross attention for semantic segmentation. In *Proceedings of the IEEE International Conference on Computer Vision*, pages 603–612, 2019.
- [21] Samvit Jain, Xin Wang, and Joseph E Gonzalez. Accel: A corrective fusion network for efficient semantic segmentation on video. In *Proceedings of the IEEE Conference on Computer Vision and Pattern Recognition*, pages 8866–8875, 2019.
- [22] Alex Kendall, Yarin Gal, and Roberto Cipolla. Multi-task learning using uncertainty to weigh losses for scene geometry and semantics. In *Proceedings of the IEEE Conference on Computer Vision and Pattern Recognition*, pages 7482–7491, 2018.
- [23] Iasonas Kokkinos. Ubertnet: Training a universal convolutional neural network for low-, mid-, and high-level vision using diverse datasets and limited memory. In *Proceedings*

- of the *IEEE Conference on Computer Vision and Pattern Recognition*, pages 6129–6138, 2017.
- [24] Yanwei Li, Xinze Chen, Zheng Zhu, Lingxi Xie, Guan Huang, Dalong Du, and Xingang Wang. Attention-guided unified network for panoptic segmentation. In *Proceedings of the IEEE Conference on Computer Vision and Pattern Recognition*, pages 7026–7035, 2019.
 - [25] Yule Li, Jianping Shi, and Dahua Lin. Low-latency video semantic segmentation. In *Proceedings of the IEEE Conference on Computer Vision and Pattern Recognition*, pages 5997–6005, 2018.
 - [26] Shikun Liu, Edward Johns, and Andrew J Davison. End-to-end multi-task learning with attention. In *Proceedings of the IEEE Conference on Computer Vision and Pattern Recognition*, pages 1871–1880, 2019.
 - [27] Jonathan Long, Evan Shelhamer, and Trevor Darrell. Fully convolutional networks for semantic segmentation. In *Proceedings of the IEEE conference on computer vision and pattern recognition*, pages 3431–3440, 2015.
 - [28] Kevis-Kokitsi Maninis, Ilija Radosavovic, and Iasonas Kokkinos. Attentive single-tasking of multiple tasks. In *Proceedings of the IEEE Conference on Computer Vision and Pattern Recognition*, pages 1851–1860, 2019.
 - [29] Ishan Misra, Abhinav Shrivastava, Abhinav Gupta, and Martial Hebert. Cross-stitch networks for multi-task learning. In *Proceedings of the IEEE Conference on Computer Vision and Pattern Recognition*, pages 3994–4003, 2016.
 - [30] David Nilsson and Cristian Sminchisescu. Semantic video segmentation by gated recurrent flow propagation. In *Proceedings of the IEEE Conference on Computer Vision and Pattern Recognition*, pages 6819–6828, 2018.
 - [31] Sebastian Ruder¹², Joachim Bingel, Isabelle Augenstein, and Anders Søgaard. Latent multi-task architecture learning. In *AAAI*, 2019.
 - [32] Ozan Sener and Vladlen Koltun. Multi-task learning as multi-objective optimization. In *Advances in Neural Information Processing Systems*, pages 527–538, 2018.
 - [33] Nathan Silberman, Derek Hoiem, Pushmeet Kohli, and Rob Fergus. Indoor segmentation and support inference from rgbd images. In *European Conference on Computer Vision*, pages 746–760. Springer, 2012.
 - [34] Raphael Tang, Weijie Wang, Zhucheng Tu, and Jimmy Lin. An experimental analysis of the power consumption of convolutional neural networks for keyword spotting. In *2018 IEEE International Conference on Acoustics, Speech and Signal Processing (ICASSP)*, pages 5479–5483. IEEE, 2018.
 - [35] Marvin Teichmann, Michael Weber, Marius Zoellner, Roberto Cipolla, and Raquel Urtasun. Multinet: Real-time joint semantic reasoning for autonomous driving. In *2018 IEEE Intelligent Vehicles Symposium (IV)*, pages 1013–1020. IEEE, 2018.
 - [36] Ashish Vaswani, Noam Shazeer, Niki Parmar, Jakob Uszkoreit, Llion Jones, Aidan N Gomez, Łukasz Kaiser, and Illia Polosukhin. Attention is all you need. In *Advances in neural information processing systems*, pages 5998–6008, 2017.
 - [37] Sanghyun Woo, Jongchan Park, Joon-Young Lee, and In So Kweon. Cbam: Convolutional block attention module. In *Proceedings of the European Conference on Computer Vision (ECCV)*, pages 3–19, 2018.
 - [38] Dan Xu, Wanli Ouyang, Xiaogang Wang, and Nicu Sebe. Pad-net: Multi-tasks guided prediction-and-distillation network for simultaneous depth estimation and scene parsing. In *Proceedings of the IEEE Conference on Computer Vision and Pattern Recognition*, pages 675–684, 2018.
 - [39] Han Zhang, Ian Goodfellow, Dimitris Metaxas, and Augustus Odena. Self-attention generative adversarial networks. *arXiv preprint arXiv:1805.08318*, 2018.
 - [40] Xizhou Zhu, Yuwen Xiong, Jifeng Dai, Lu Yuan, and Yichen Wei. Deep feature flow for video recognition. In *Proceedings of the IEEE Conference on Computer Vision and Pattern Recognition*, pages 2349–2358, 2017.
 - [41] Barret Zoph, Vijay Vasudevan, Jonathon Shlens, and Quoc V Le. Learning transferable architectures for scalable image recognition. In *Proceedings of the IEEE conference on computer vision and pattern recognition*, pages 8697–8710, 2018.